THE JOURNAL OF COMPARATIVE NEUROLOGY 445:13–28 (2002)

Effects of Age on the Glial Cells in the Rhesus Monkey Optic Nerve

JULIE H. SANDELL* AND ALAN PETERS
Department of Anatomy and Neurobiology, Boston University School of Medicine, Boston, Massachusetts 02118

ABSTRACT

The optic nerve is a circumscribed white matter tract consisting of myelinated nerve fibers and neuroglial cells. Previous work has shown that during normal aging in the rhesus monkey, many optic nerves lose some of their nerve fibers, and in all old optic nerves there are both myelin abnormalities and degenerating nerve fibers. The present study assesses how the neuroglial cell population of the optic nerve is affected by age. To address this question, optic nerves from young (4–10 years) and old (27–33 years) rhesus monkeys were examined by using both light and electron microscopy. It was found that with age the astrocytes, oligodendrocytes, and microglia all develop characteristic cytoplasmic inclusions. The astrocytes hypertrophy and fill space vacated by degenerated nerve fibers, and they often develop abundant glial filaments in their processes. Oligodendrocytes and microglial cells both become more numerous with age, and microglial cells often become engorged with phagocytosed debris. Some of the debris can be recognized as degenerating myelin, and in general, the greater the loss of nerve fibers, the more active the microglial cells become. J. Comp. Neurol. 445:13–28, 2002.

Indexing terms: aging; primate; astrocyte; oligodendrocyte; microglia; electron microscopy

In a previous article we described the effects of age on the nerve fibers in the optic nerve of the rhesus monkey (Sandell and Peters, 2001). The present article continues this study and describes the effects of age on the neuroglial cells in the same nerves.

When the optic nerves of young monkeys, 4–10 years of age, are compared with those of monkeys that are over 27 years old, the old monkeys as a group show a loss of about 45% of their nerve fibers. However, the extent of nerve fiber loss from the optic nerves of the old monkeys is variable. In some old monkeys the numbers of nerve fibers are comparable to those in young monkeys, but in the most affected old nerves, almost 75% of the fibers are lost.

Several other studies have also detected a loss of nerve fibers from the optic nerves of both old humans (Balazsi et al., 1984; Mikelberg et al., 1989; Jonas et al., 1992) and old monkeys (Morrison et al., 1990), but our previous study is the only one in which the age-related changes in the structure of the nerve fibers have been examined in detail. Two types of changes were observed. One is the normal effect of age on the structure of the myelin sheaths, and the other is the degeneration of axons and their myelin sheaths. The age-related alterations in the myelin sheaths of optic nerve fibers are similar to those encountered in other parts of the central nervous system (e.g., Feldman and Peters, 1998; Peters, 1999; Peters et al., 2000), with the most common being a splitting of the sheath at the major dense line to accommodate electron-dense cytoplasm that is derived from the parent oligodendrocyte. Other, less frequent, age-related alterations are splitting of the intraperiod line to accommodate an accumulation of fluid, so that the sheath balloons out at that site, and the formation of myelin sheaths that are too large for the enclosed axon. In the optic nerves most affected by age, degeneration of some of the nerve fibers is superimposed on these normal age-related changes in myelin.

Of course it is this degeneration of nerve fibers that leads to the reduced numbers of nerve fibers in old optic nerves, and it may be that loss of nerve fibers from the white matter is a normal consequence of aging in all parts of the central nervous system. For example, by using magnetic resonance imaging, a global age-related loss of subcortical white matter has been observed in normal

Grant sponsor: National Institutes of Health, National Institute on Aging; Grant number: 2PO1 AG00001.

*Correspondence to: Julie H. Sandell, Ph.D., Department of Anatomy and Neurobiology, 715 Albany Street, Boston, MA 02118.
E-mail: jsandell@cajal-1.bu.edu

Received 30 May 2001; Revised 28 August 2001; 10 December 2001

DOI 10.1002/cne.10162

humans and monkeys (Albert, 1993; Lai et al., 1995; Guttmann et al., 1998), whereas Tang and colleagues (1997) have used stereology to show that there is an age-related 27% decrease in the total length of nerve fibers in the white matter of human cerebral hemispheres.

Aging affects not only the nerve fibers in the optic nerve but also the neuroglial cells that support them. It can be presumed that the oligodendroglia must be directly affected by the changes in the nerve fibers because they are the cells responsible for the formation and maintenance of the myelin sheaths. It is known that in the aging cerebral cortex, oligodendrocytes develop distinctive inclusions, some of which occupy swellings of their processes (Peters, 1996). In addition, microglia are involved in the phagocytosis of degenerating optic nerve fibers (Sandell and Peters, 2001), and several studies have detected microglial activation in the subcortical white matter of aging monkeys (Sheffield and Berman, 1998; Sloane et al., 1999). Astrocytes are also affected by age. They become enlarged and increase their production and degradation of glial fibrillary acidic protein (GFAP; Linnemann and Skarsfelt, 1994; Sloane et al., 2000).

The present study was undertaken to learn more about the involvement of the neuroglial cells in the aging of the optic nerve and to determine how the structure and numbers of neuroglial cells alter with age. The optic nerve provides an excellent model system in which to investigate the normal age-related changes that occur in the neuroglial cells of the white matter, because it is a well circumscribed central nervous system tract upon which both morphological and quantitative analyses can be carried out.

MATERIALS AND METHODS

Tissue specimens and processing

These studies used optic nerves from rhesus monkeys (*Macaca mulatta*). The same specimens were used to examine the effects of age on nerve fibers in the rhesus monkey optic nerve, and details regarding the animal population have been published (Sandell and Peters, 2001). In brief, optic nerves were obtained from seven young monkeys (4–10 years of age, total of 13 nerves) and six old monkeys (27–33 years of age, total of 11 nerves). Three old monkeys (AM 062, 065, and 091) received ophthalmoscopic examinations by Dr. Alcides Fernandes at the Yerkes Regional Primate Center in Atlanta, Georgia. All three had some degree of cataract; AM 062 and 065 had normal intraocular pressure, which was not measured in AM 091; and AM 065 had some retinal pigment epithelium atrophy near the macula. No other significant age-related changes were noted. The retinae of AM 041 were examined post mortem by Dr. Edward Chaum at Boston Medical Center. The only age-related findings were mild drusen and peripheral cystoid changes, consistent with an equivalent human age of 96. The procedures used for tissue preparation have been previously described (Peters et al., 1994; Peters et al., 2000; Sandell and Peters, 2001). All procedures regarding the care and euthanasia of these animals were approved by the Institutional Animal Care and Use Committee of Boston University School of Medicine and were in accordance with the National Research Council publication *Guide for the Care and Use of Laboratory Animals*.

For perfusion the animals were preanesthetized with ketamine (10 mg/kg) and further anesthetized to a state of areflexia with intravenous sodium pentobarbital (35 mg/kg). The anesthetized animals were artificially respired with 95% oxygen and 5% carbon dioxide and perfused transcardially with 4 liters of warm fixative (1% paraformaldehyde and 1.25% glutaraldehyde in 0.1 M phosphate or 0.1 M cacodylate buffer at pH 7.4). The eyes were removed, with a segment of the optic nerve attached that was approx. 4 mm in length. Several smaller pieces, each approx. 1–2 mm in length, were cut from this 4-mm segment of each nerve and were stored in the cold in a stronger fixative (2% paraformaldehyde and 2.5% glutaraldehyde in 0.1 M phosphate or 0.1 M cacodylate buffer, pH 7.4) until further processing. The segments of optic nerve were osmicated, dehydrated in ascending concentrations of ethanol, and embedded in Araldite. Transverse, 1-μm semithick sections were collected and stained with toluidine blue for light microscopic studies. Thin sections were taken for electron microscopy, stained with uranyl acetate and lead citrate, and subsequently examined in a JEOL 100 electron microscope.

Glial nuclear profile counts/light microscopy

An estimate of the total number of neuroglial nuclear profiles was made from transverse sections of each optic nerve. The sections were stained with toluidine blue and analyzed by using the Bioquant BQ-TCW-95 system (R&M Biometrics, Nashville, TN) and a motorized stage. A section was viewed with a 100× oil immersion objective (NA 1.40) and the image projected onto a video monitor. The counting of glial nuclear profiles was done simultaneously by both authors, and the computer system was used to generate the counting grid, move the stage, project the counting box onto the video image, mark the profiles as they were counted, tally the counts, and calculate the cross-sectional area of the nerve. The counting boxes were 30×30 μm each, spaced 200 μm from center to center in a grid that was placed randomly on the section of the nerve. All neuroglial cell profiles displaying nuclei were counted in each counting box, provided that they did not intersect the forbidden margins of the counting box (left side and bottom). Profiles of fibroblasts, endothelial cells, and pericytes were not counted. The counting was done without explicit knowledge of the ages of the nerves, although in many old nerves the changes in nerve fibers and neuroglial cells were obvious.

The counting parameters, such as counting box size, grid spacing, and number of counting boxes, were determined empirically to yield coefficients of error (CE = SEM/mean) within the 10% recommended by West and colleagues (1996) for design-based analysis. The CE values calculated for each nerve ranged from 7.1 to 9.8%. The estimated total number of glial nuclear profiles present in a transverse section of each nerve was determined by simply multiplying the mean number of profiles/mm^2 by the cross-sectional area of the nerve.

Size of glial nuclear profiles

A separate analysis of 1-μm-thick transverse sections from the same nerves was performed to determine whether the sizes of the neuroglial nuclear profiles change with age. This information was used in calculations to determine whether changes in nuclear size might contribute to apparent changes in profile number, when neuro-

TABLE 1. Quantitative Analyses of Optic Nerves

Age, sex	ID no., optic nerve	Total fibers[1]	Area[2] (mm^2)	Glial profiles/mm^2	Est. total glial profiles	Glia/ fiber	% Astrocytes	% Microglial cells	% Oligodendrocytes	Est. astro. profile/sec	Est. micro. profile/sec	Est. oligo. profile/sec
Young												
4, M	AM058, right	1692379	7.332	703	5,154	0.00305						
4, M	AM058, left	1514860	5.401	674	3,640	0.00240	30	2	68	1,092	73	2,475
5, M	R419, left	1470878	5.557	577	3,207	0.00218						
5, M	R419, right	1507763	5.273	605	3,190	0.00212	39	5	56	1,244	160	1,786
6, F	AM076, left	1335603	6.508	449	2,922	0.00219						
6, F	AM076, right	1431711	6.044	469	2,835	0.00198	28	6	66	7,94	170	1,871
6, F	AM077, left	1581199	5.495	488	2,681	0.00170						
6, F	AM077, right	1694823	5.968	583	3,479	0.00205	40	5	55	1,392	174	1,913
9, F	AM097, left	2061735	6.400	562	3,232	0.00157	37	8	55	1,196	258	1,778
9, F	AM097, right	2066343	6.370	509	3,243	0.00157						
9, M	AM047, right	1697390	6.819	522	3,559	0.00210	31	8	61	1,103	285	2,171
10, M	AM053, left	1627496	5.097	754	3,843	0.00236						
10, M	AM053, right	1541652	6.353	411	2,611	0.00169	40	7	53	1,044	183	1,384
Mean		**1,632,600**	**6.048**	**562**	**3,354**	**0.00207**	**35**	**6**	**59**	**1,124**	**186**	**1,911**
Old												
27, M	AM062, left	999820	6.605	850	5,613	0.00561	23	8	69	1,291	449	3,873
29, F	AM026, right	912342	5.538	846	4,684	0.00513						
29, F	AM026, left	974749	5.361	863	4,627	0.00475	31	6	63	1,434	278	2,915
32, M	AM091, right	712036	5.248	801	4,204	0.00590	30	8	62	1,261	336	2,606
32, M	AM091, left	635159	5.060	902	4,564	0.00719						
32, F	AM041, left	384044	3.864	1,200	4,636	0.01207	25	35	40	1,159	1,623	1,854
32, F	AM041, right	410499	3.620	1,388	5,023	0.01224	25	26	49	1,256	1,306	2,461
							($\bar{X}$ = 25)	($\bar{X}$ = 30.5)	($\bar{X}$ = 44.5)	($\bar{X}$ = 1270.5)	($\bar{X}$ = 1464.5)	($\bar{X}$ = 2157.5)
32, F	AM023, right	679475	4.567	654	2,987	0.00440						
32, F	AM023, left	1306000	6.141	643	3,949	0.00302	26	4	70	1,027	158	2,764
33, F	AM065, left	1481563	7.005	681	4,771	0.00322						
33, F	AM065, right	1485347	6.477	435	2,818	0.00190	38	6	56	1,071	169	1,578
Mean		**907370**	**5.408**	**842**	**4,352**	**0.00595**	**29**	**10**	**61**	**1,225**	**476**	**2,649**
Two-tailed P, young vs. old		0.001	0.20 (ns)	0.02	0.01	0.01	0.06	0.45 [ns (M-W)]	0.72 (ns)	0.31 (ns)	0.23 [ns (M-W)]	0.07 [ns (M-W)]

[1]Fiber numbers from Sandell and Peters, 2001.
[2]Areas from current study.
[3]M-W, Mann-Whitney test.

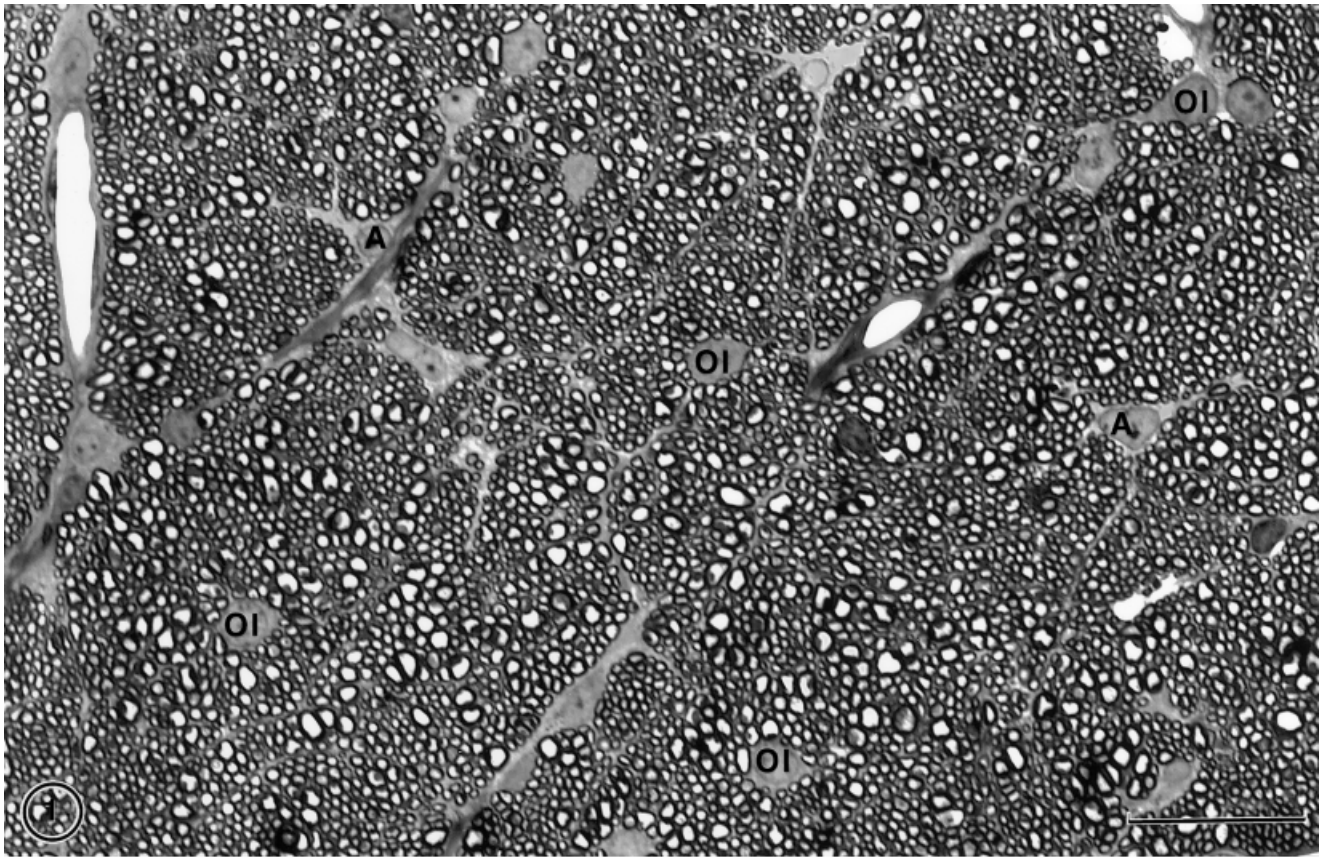

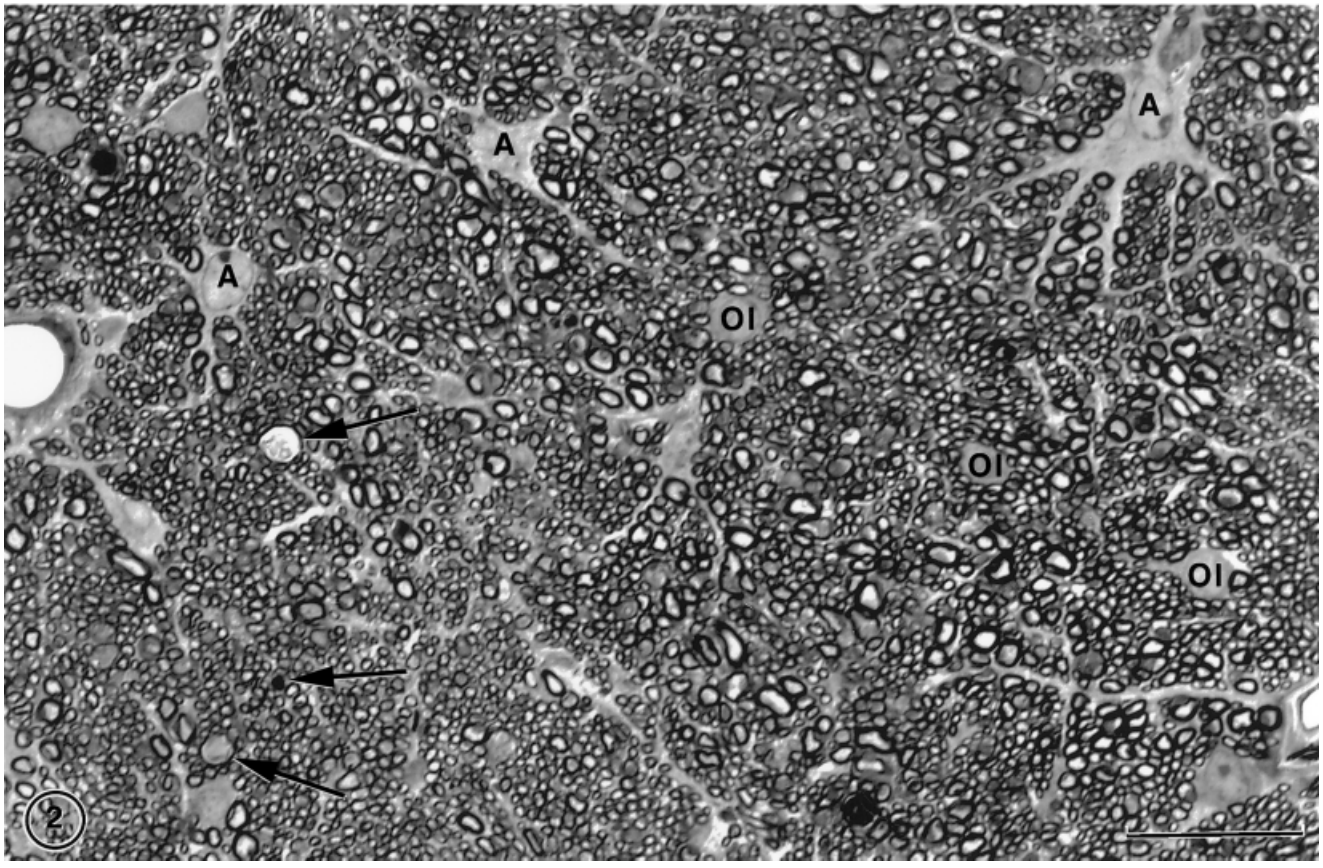

Figures 1–2

glial profile counts in young and old nerves were compared (see Results). For each nerve, at least 70 neuroglial nuclear profiles of each cell type (astrocytes, oligodendrocytes and microglia) were drawn by using a camera lucida and a 100× objective. The drawings were scanned and digitized by using Adobe Photoshop 4.0, and the area of each profile was determined by using NIH Image software. The mean areas were used to calculate mean diameters, assuming that the nuclei were spherical. This is a simplification for astrocytes and microglia but is fairly accurate for oligodendrocytes.

Relative proportions of glial nuclear profile types/electron microscopy

Thin sections from one optic nerve of each of the monkeys were examined by electron microscopy to determine the relative proportions of astrocytes, oligodendrocytes, and microglia present within the nerve. The nerves were chosen on the basis of superior fixation. Both nerves from AM041, the most severely affected old monkey, were examined. For each optic nerve, a total of at least 200 consecutive neuroglial cells that displayed profiles of their nuclei were identified on the basis of their intracellular morphology and staining characteristics. From this analysis of the relative percentages of each neuroglial cell type within the optic nerves of each monkey, the total number of profiles of each type of neuroglial cell in cross sections of the nerves were estimated (Table 1). However, because the sizes of the nuclei of the three neuroglial cell types are not the same, this only provides a rough estimate of the proportions of the three neuroglial cell types. Thin sections of the optic nerves were also examined to ascertain the presence and characteristics of age-related changes in the neuroglial cells.

Statistical analysis

For statistical purposes the optic nerves were divided into two groups. "Young" designates nerves from animals that were ≤10 years old, and "old" designates nerves from animals that were ≥27 years old. The data are presented in Table 1. Because counts from the two optic nerves from a single animal are not statistically independent measures, we used mixed linear models to account for the within-subject correlation in the data (Diggle et al., 1994). In each analysis we assumed a working correlation structure of compound symmetry. All significance values were obtained from two-tailed tests, on the assumption that we could not predict a unidirectional effect of age on any variable. Linear correlation analyses were used to assess the relationship between neuroglial nuclear profile data obtained in the present study and data on nerve fiber counts obtained for the same nerves in our previous study (Sandell and Peters, 2001). These analyses were also adjusted for within-subject correlation by using the mixed model method (Diggle et al., 1994).

The studies of individual glial cell types used only one nerve per animal, except for AM 041, the most affected old animal. Student's t-tests were used to analyze data regarding individual glial cell types, and for this analysis the data from the two nerves of AM 041 were averaged. The Mann-Whitney U test was used to evaluate differences between the two groups if the difference in the standard deviation of the two data sets suggested that a nonparametric test was more appropriate. Use of this nonparametric test is indicated by M-W in Table 1.

RESULTS

Morphological observations

In the rhesus monkey, the optic nerve is about 3 mm in diameter, and in young specimens it contains closely packed nerve fibers, which are partially segregated into bundles by connective tissue trabeculae that contain the blood vessels supplying the nerve. The neuroglial cells (astrocytes, oligodendrocytes, and microglia) are interspersed among the nerve fibers. Unfortunately, because of the sparsity of blood vessels, the fixation of the nerve fibers and neuroglial cells in these optic nerves is usually less than optimal. Consequently, it is common for nerve fibers to have splits and shears in their myelin sheaths, for the processes of astrocytes to be swollen, and for their cytoplasm to contain swollen mitochondria. However, in the nerves we chose to include in this study, the fixation was more than adequate for our analysis of the effects of age on the neuroglial cells.

The appearance of a typical young optic nerve is illustrated in Figure 1 (AM 053, 10 years old). The myelinated nerve fibers are tightly packed, and generally the neuroglial cell nuclei are surrounded by very little cytoplasm. The optic nerves of AM 065, which is a 33-year-old monkey that appears to have lost few nerve fibers, look very similar to those of young monkeys. However, in the optic nerves of some old monkeys, such as AM026 (29 years old; Fig. 2) from which approximately 40% of the nerve fibers have been lost (Sandell and Peters, 2001), the packing of the nerve fibers is obviously looser, and some axons are degenerating (indicated by arrows). In those optic nerves that show the most extensive loss of nerve fibers, such as AM041, which is 32 years old and has lost some 75% of the nerve fibers (Sandell and Peters, 2001), the depletion of nerve fibers is very obvious, but the loss is patchy (Figs. 3, 4). Consequently, in some parts of this optic nerve the fibers are still relatively closely packed, but separated into small fascicles by an extensive network of astrocytic processes (Fig. 3). However, in the more severely depleted areas, the dominant structures are degenerating axons and neuroglial cells, many of which are microglia that contain phagocytosed material (Fig. 4, M).

Neuroglial subtypes

Astrocytes. In semithick sections from young optic nerves stained with toluidine blue, the astrocytes are recognized by their pale, often irregularly shaped nuclei that

Fig. 1. Semithick section of the optic nerve of a 10-year-old monkey, AM 053. In this young optic nerve the nerve fibers are tightly packed, and distributed among them are the pale, star-shaped profiles of astrocytes (As), the darker profiles of oligodendrocytes with rounded nuclei (Ol), and an occasional microglial cell, with a small, dark nucleus and dark cytoplasm. Scale bar = 25 μm.

Fig. 2. Semithick section of the optic nerve of a 29-year-old monkey, AM 026.This optic nerve has lost some nerve fibers, and a few profiles of degenerating nerve fibers are apparent (arrows). Compared with young optic nerves (Fig. 1), there is little change in the appearance of the oligodendroglial cells (Ol) with age, but the astrocytes (A) have hypertrophied so that they have larger cell bodies and thicker processes. Scale bar = 25 μm.

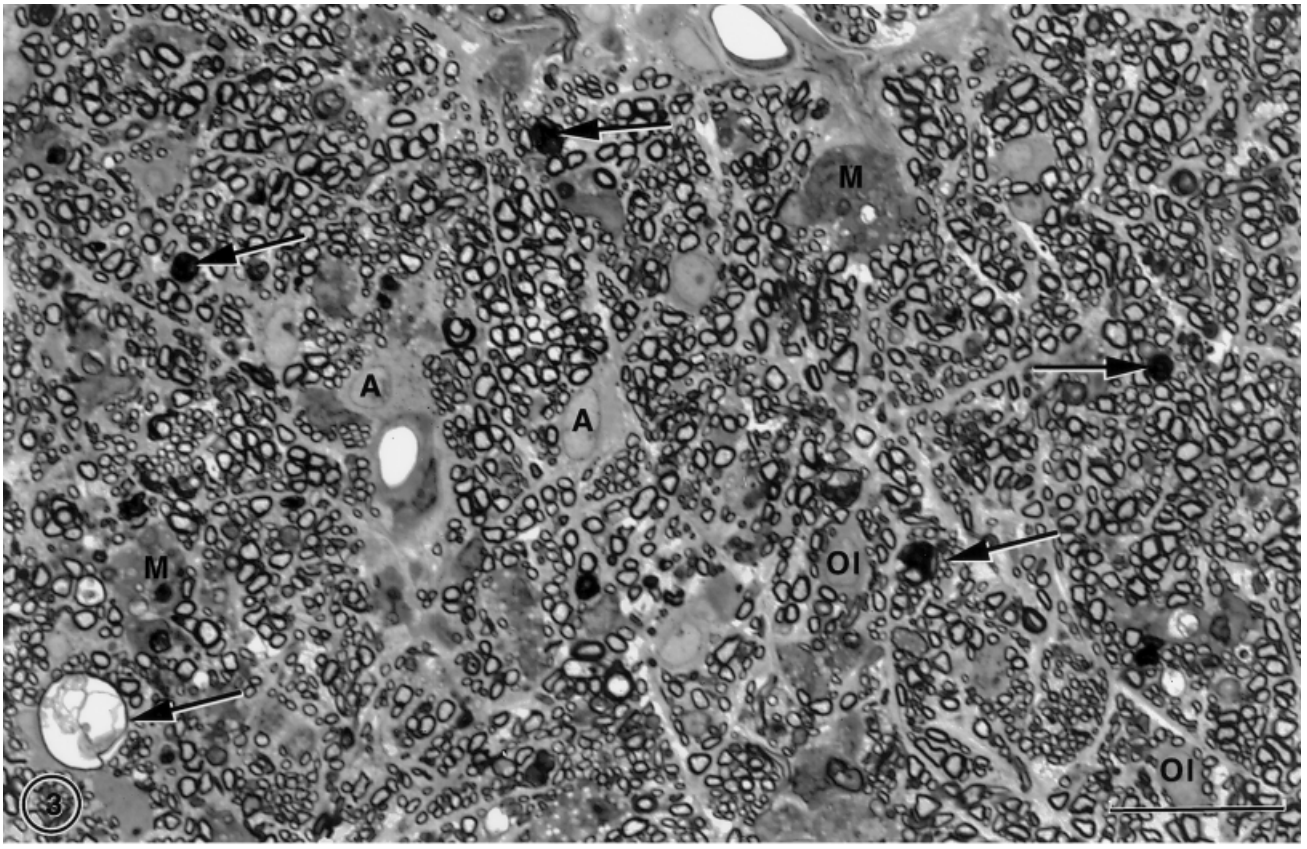

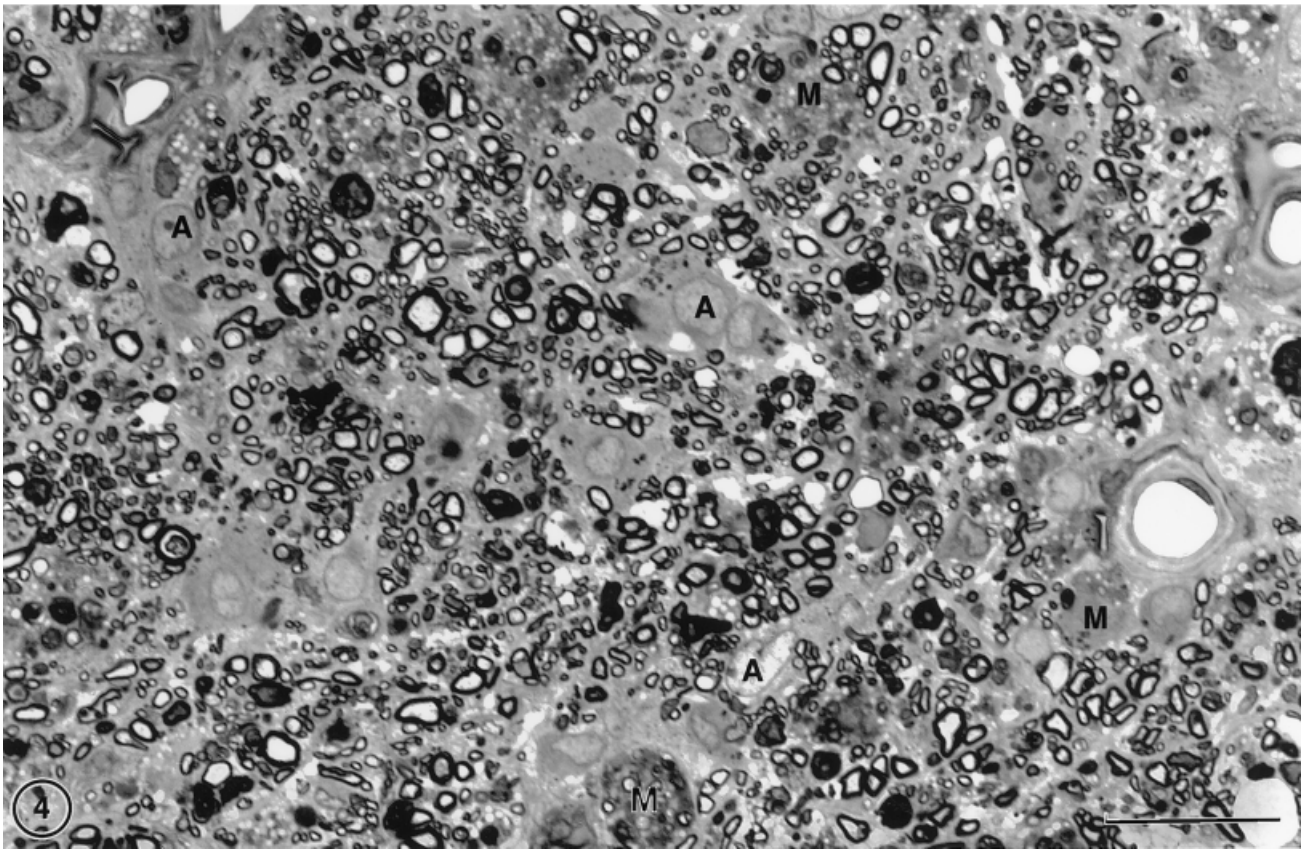

Figures 3–4

sometimes display a rather large and dark nucleolus (Fig. 1A). Surrounding the nucleus is an even paler perikaryon, from which processes radiate out between the surrounding nerve fibers to give the astrocytes their typical star-shaped profiles. In the optic nerves of most of the old monkeys, the astrocytes are more prominent (Fig. 2, AM 026; Figs. 3 and 4, AM 041). Their perikarya are larger than in young nerves and their processes are thicker, endowing the astrocytes with an even more pronounced star shape. Also, because the astrocyte processes are thickened, the sheets of processes passing between nerve fibers are much more obvious in the older optic nerves.

In thin sections the nuclear envelope of the astrocytes frequently appears infolded, and the perikaryon molds itself to the contours of the surrounding nerve fibers (Fig. 5, AM 077, 6 years old). Bundles of filaments (f) pass through the organelle-sparse pale cytoplasm of the cell body to enter the processes (P), some of which aggregate with those of other astrocytes to form sheets that pass between bundles of nerve fibers. Both at the periphery of the optic nerve and at the interface with the fibrous trabeculae, processes of astrocytes form a complete glial limiting membrane that separates the nerve fibers from other tissues. In old optic nerves, the cytoplasm of the astrocytes is voluminous and contains vacuoles, and in some cases phagocytosed material; astrocytic processes contain abundant filaments, and swollen astrocytic processes (P) are common (Fig. 8).

Oligodendrocytes. In sections from young optic nerves, the oligodendrocytes are the most common of the neuroglial cell profiles (Fig. 1, Ol). These cells form the myelin sheaths of the nerve fibers. In semithick sections the nuclei of the oligodendrocytes generally have rounded profiles and because they contain more heterochromatin than the astrocytes, their nuclei are stained more darkly and unevenly. In both light and electron microscopic preparations, the cytoplasm of the oligodendrocytes also stains more darkly than that of the astrocytes; the contours of the perikarya of the oligodendrocytes are rounded, and it is not common to see processes extending from them (Figs. 1, 7). In electron micrographs the rough endoplasmic reticulum (ER) of the oligodendrocytes is sparse and consists of rather short cisternae that often occur singly (Fig. 7) but can be arranged to form small stacks.

In old optic nerves, the oligodendrocytes appear to be little affected by age, as viewed by light microscopy (Figs. 2–4, Ol). However, in electron microscopic preparations (Figs. 8, 9) some of the oligodendrocytes can be seen to have thick processes extending from their cell bodies, and both oligodendrocyte cell bodies and their processes frequently contain electron-dense inclusions (Fig. 9I).

Microglial cells. The least common of the neuroglial cells in young monkeys are the microglia. In both light (Fig. 1) and electron micrographs (Fig. 6), their nuclei can be seen to be smaller, darker, and often elongated compared with those of the oligodendrocytes. However, in its staining characteristics the perikaryal cytoplasm of the microglial cell is very similar to that of the oligodendrocyte. But the cell bodies of the microglial cells generally have more elongated irregular profiles, and the cisternae of the rough endoplasmic reticulum (ER) are longer. It is not uncommon to encounter lysosomes and inclusions in the cytoplasm of microglial cells, even in young monkeys (Fig. 6I).

In old optic nerves, especially in those with the most severe depletions of nerve fibers, the most obvious change is in the microglial cell population. The numbers of microglial cells increase compared with the nerves of young monkeys, and even in light microscopic preparations it can be seen that many of the cell bodies of the microglial cells have become greatly enlarged and their dark cytoplasm contains vacuoles and dense inclusions (Figs 3 and 4, M). In thin sections (Figs. 8–10), it is evident that many of these inclusions are derived from phagocytosed myelin sheaths, because the alternating major dense and intraperiod lines can be discerned within some of the lamellar inclusions. These inclusions are distinct from those in the other glial cell types, because in oligodendrocytes and astrocytes the inclusions are rarely lamellar. In addition to the membraneous inclusions, other phagocytosed contents of the microglial cells are granular and electron-dense, and they sometimes contain vesicles and vacuoles (Fig. 10). Some of these inclusions may be of neuronal origin, because in severely affected old nerves some of the nerve fibers show degenerating axons with dense cytoplasm (Fig. 8, N_1), whereas in others the axons have completely disappeared, so that only a degenerating myelin sheath remains (Fig. 8, N_2).

Quantitative analyses

Numbers and density of neuroglial cell nuclear profiles. We observed a 30% increase in the mean total number of neuroglial cell nuclear profiles in transverse sections of the optic nerves of old monkeys (mean ± SEM: 4,352 ± 251) compared with young monkeys (mean ± SEM: 3,354 ± 182, two-tailed $P = 0.01$). Although the group difference between young and old nerves is robust, there is considerable variability in the neuroglial cell populations within both the young and old nerves, as shown in Figure 11 and Table 1. The density of glial cell nuclear profiles per mm^2 is also higher in the old nerves (mean density/mm^2 ± SEM for old: 842 ± 80; for young: 562 ± 28; two-tailed $P = 0.02$), even though there is no significant difference in the cross-sectional areas of the optic nerves in young and old monkeys (Table 1).

Fig. 3. Semithick section of the optic nerve of a 32-year-old monkey, AM 041. In this portion of the optic nerve, there has been an obvious loss of nerve fibers, and profiles of degenerating nerve fibers are frequent (arrows). There appears to be little change in the oligodendrocytes (Ol), but the astrocytes (A) have hypertrophied to produce an extensive network of pale processes passing between the remaining nerve fibers. Some microglial cells are relatively normal (m), whereas others have become reactive (M). The reactive cells are enormously enlarged and have vacuoles and dark inclusions in their cell bodies. Scale bar = 25 μm.

Fig. 4. Semithick section through another portion of the optic nerve of AM 041, a 32-year-old monkey. In this portion of the nerve the degeneration is even more pronounced than that illustrated in Figure 3. Although some profiles of astrocytes (A) can be recognized by their pale, irregularly shaped nuclei surrounded by a pale cytoplasm, it is more difficult to distinguish between oligodendrocytes and unreactive microglial cells. However, reactive microglial cells (M) are easily identified because of their swollen cell bodies that contain vacuoles and dark inclusions. Scale bar = 25 μm.

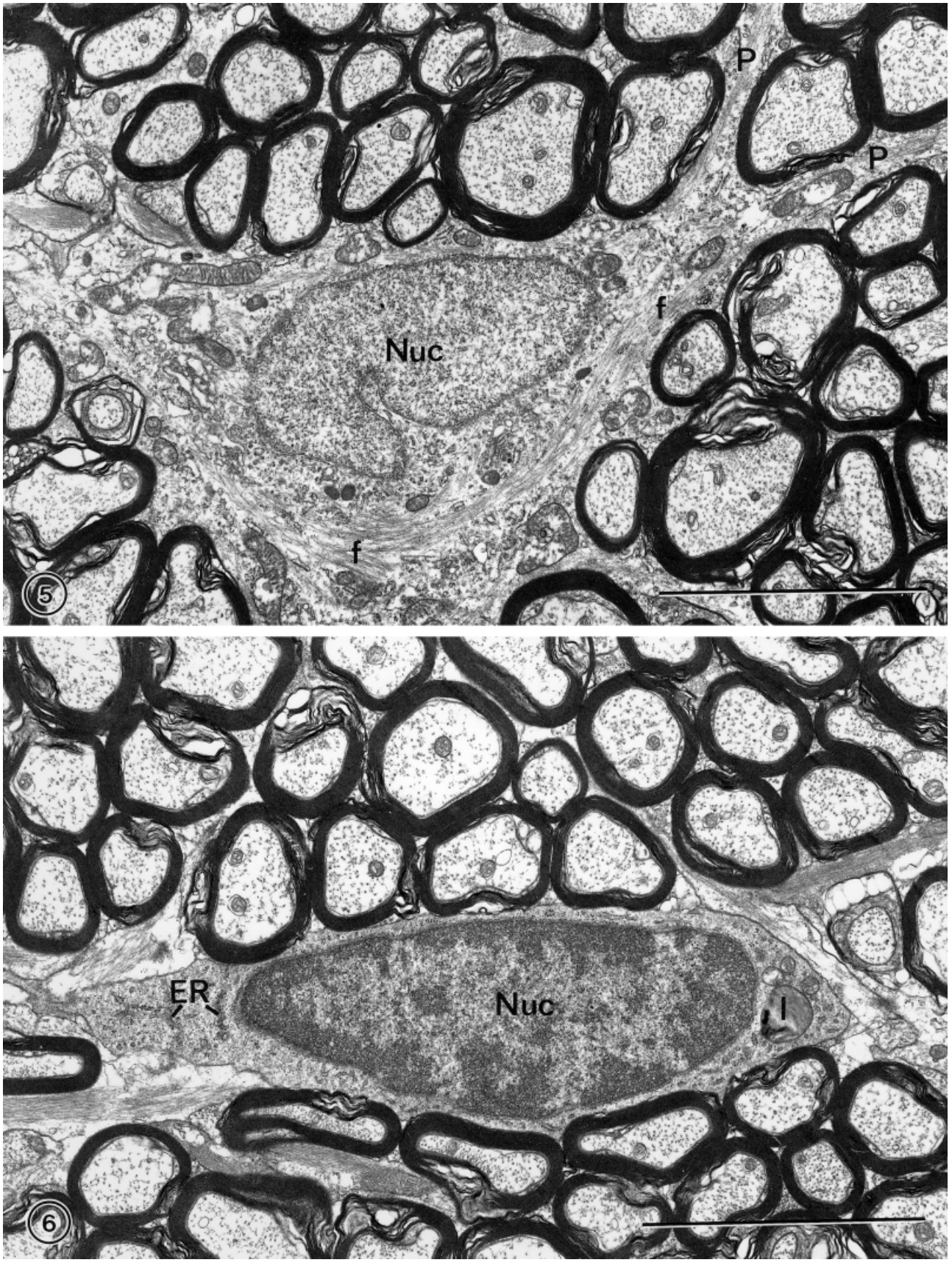

Figures 5–6

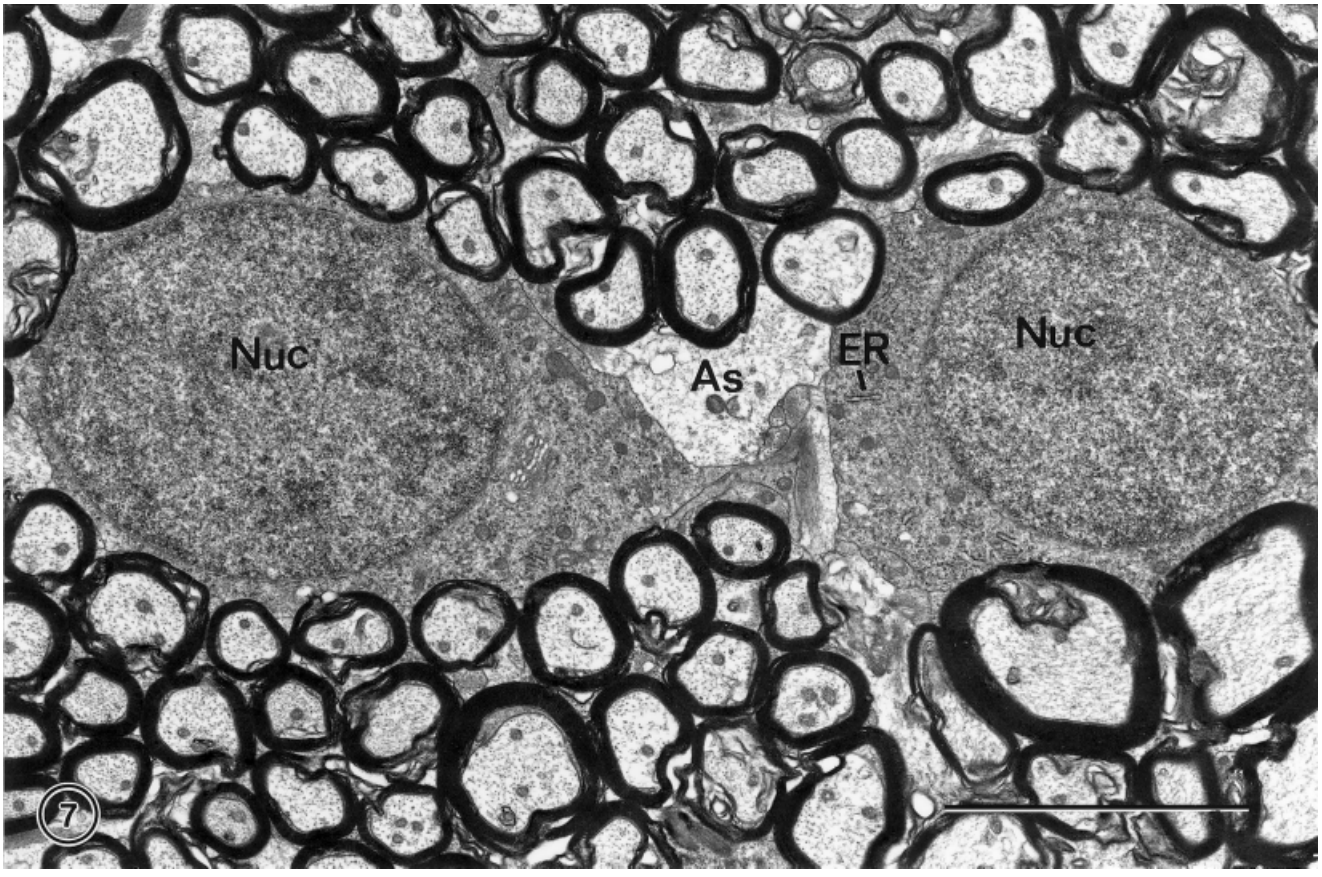

Fig. 7. Electron micrograph of oligodendrocytes in the optic nerve of a 10-year-old monkey, AM 053. The oligodendrocytes have dark, rounded nuclei (Nuc).The cytoplasm is much darker than that of astrocytes (As) and contains a few short cisternae of endoplasmic reticulum (ER). Scale bar = 5 μm.

Relationship between neuroglial nuclear profile counts and fiber counts. The total number of neuroglial nuclear profiles is negatively correlated with the number of nerve fiber profiles in the optic nerve, as shown in Figure 12 ($r = -0.4957$, $P = 0.03$). Thus the nerves with the most fibers (which come from young animals) have fewer neuroglial nuclear profiles, and the nerves with fewer fibers (which tend to come from older animals) have more neuroglial nuclear profiles. The consequence is that the ratio of neuroglial nuclear profiles to nerve fiber profiles is significantly increased in the old optic nerves: 0.0021:1 for young nerves; 0.0060:1 for old nerves, two-tailed $P = 0.01$).

Proportions of neuroglial cells in individual nerves. The proportions of the different neuroglial nuclear subtypes in each nerve are shown in Figure 13 and Table 1. A relatively well-preserved old nerve, such as that of AM 065 (33 years old), is indistinguishable from young nerves in terms of the proportions of the various neuroglial nuclei that can be identified, whereas in the nerves most affected by age (AM041), there is a massive increase in the proportion of microglial nuclear profiles. Even though the estimated total *number* of oligodendrocyte profiles in transverse sections of the nerves of AM 041 is similar to that of other nerves (Table 1), there is a reduction in the *proportion* of oligodendrocytic nuclear profiles because of the much greater frequency of microglial cell profiles. Overall, in the old animals, there is a slight decrease in the percentage of astrocytes, a slight increase in the percentage of microglia, and little change in the proportion of oligodendrocytes. None of these group changes are statistically significant.

Calculated numbers of each of the neuroglial nuclear profile subtypes. Although there is an increase in the mean estimated number of each cell type in the old animals, none of the increases are statistically significant (Table 1), perhaps because the sample sizes are small.

Fig. 5. An electron micrograph of an astrocyte in the optic nerve of a 6-year-old monkey, AM 077. Astrocytes have a pale, irregularly shaped nucleus (Nuc). The pale cytoplasm contains bundles of filaments (f), and these cells generate an extensive network of processes (P) that pass between nerve fibers. Scale bar = 5 μm.

Fig. 6. Electron micrograph of a microglial cell in the optic nerve of a 6-year-old monkey, AM 077. The nucleus (Nuc) of this microglial cell is elongate and contains more clumped chromatin than that of an oligodendrocyte, but the cytoplasm of the two cell types is of similar density. However, microglial cells have longer cisternae of rough endoplasmic reticulum (ER) than oligodendrocytes and frequently contain inclusions (I). Scale bar = 5 μm.

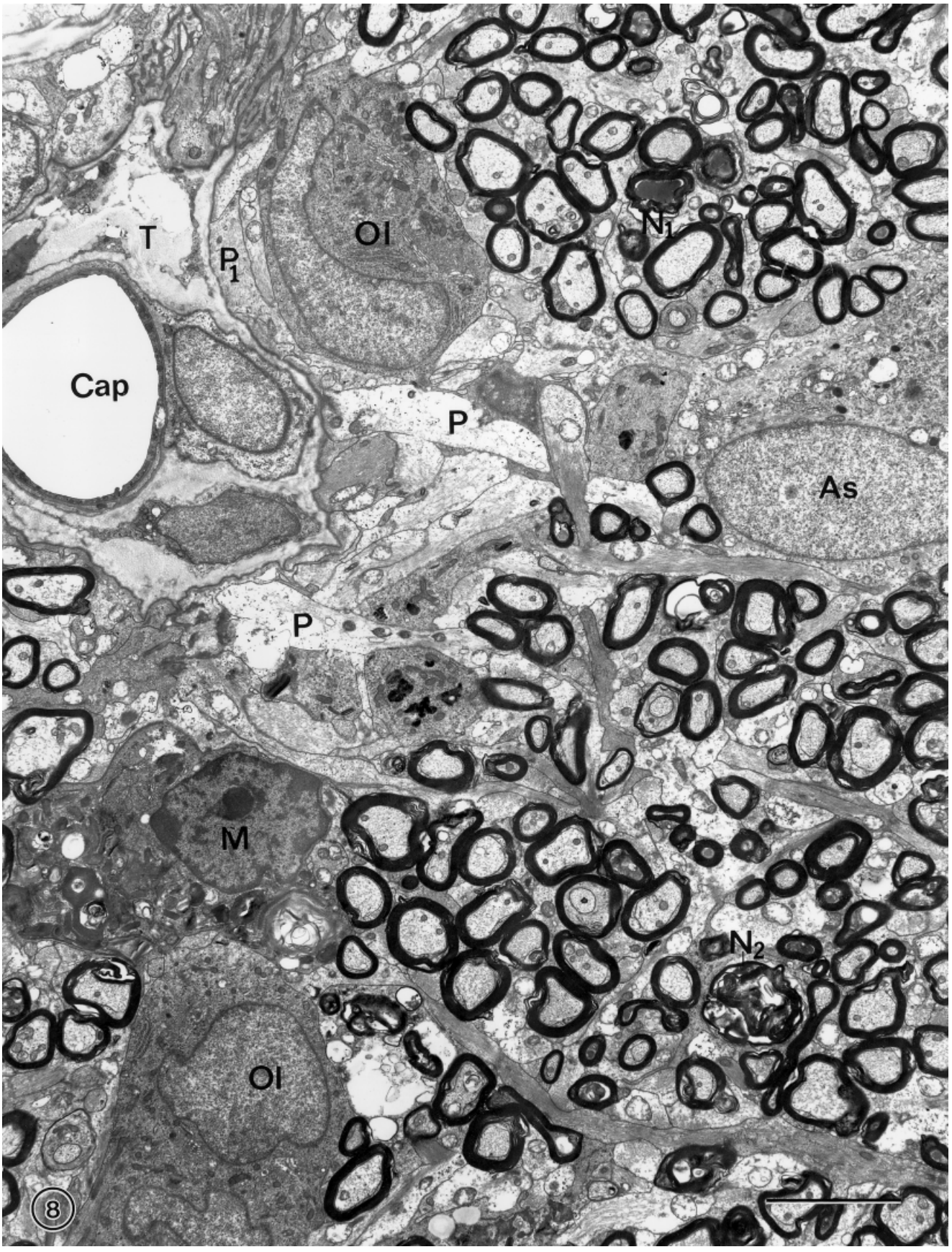

Fig. 8. A low-power electron micrograph of part of the optic nerve of a 32-year-old monkey, AM 041. Some of the nerve fibers appear normal, but others have axons with dense cytoplasm (N_1) and yet others (N_2) have lost their axons and consist of only degenerating myelin. The astrocyte (As) in the field has a voluminous cytoplasm. Pale processes of astrocytes (P) both pass between the nerve fibers and form the glial limiting membrane (P_1), which separates the nerve fibers from the trabeculae (T) that contain collagen and the capillaries (Cap). The two oligodendrocytes (Ol) in the field seem to be relatively unaltered, but the microglial cell (M) has numerous inclusions in its cytoplasm. Scale bar = 25 μm.

However, because the age-related increase in the number of microglial cells and oligodendrocytes could not be accounted for by increased profile size (see below), it can be concluded that there is a real trend toward increased numbers of these cells in old optic nerves.

Sizes of neuroglial nuclear profiles. Because nuclear profiles are used as the counting objects in this study, it is necessary to determine whether the sizes of the nuclei change with age, and if they do, what effect this has on the profile counts. The age-related increase in nuclear profile diameter in the optic nerve is 7.3% for astrocytes, 1.6% for oligodendrocytes, and 5.3% for microglia. In the case of astrocytes, the difference between the total number of profiles displayed by the young and old nerves can be accounted for solely by an increase in the size of the profiles, because the number of profiles in the young nerves (1,124, Table 1) multiplied by 1.073 equals 1,206, which is very close to the number of profiles obtained in the old nerves (1,225, Table 1). For oligodendrocytes, the increase in profile size has less impact, because the number of profiles in the young nerves (1,911, Table 1) multiplied by 1.016 equals 1,942, which is much less than the number of profiles in the old nerves (2,649, Table 1). Likewise, for microglia the increase in profile size only accounts for a small part of the increase in profile number, because the mean number of profiles in the young nerves (186, Table 1) multiplied by 1.053 equals 196, which is again much less than the mean number of profiles in the old nerves (476, Table 1). Although the various assumptions inherent in this analysis do not allow definitive conclusions to be drawn about changes in neuroglial cell number, it is clear that more nuclear profiles of microglia and oligodendroglia are encountered in the sections of the old optic nerves than can be accounted for simply on the basis of an age-related increase in the sizes of their nuclei.

DISCUSSION

In many ways, the optic nerve is like any other white matter tract in the central nervous system. The different kinds of neuroglia have specific functions, and each reacts somewhat differently to aging. Oligodendrocytes invest each retinal ganglion cell axon with a myelin sheath, and with age myelin sheaths develop vacuoles and inclusions of dark cytoplasm within the sheaths. Astrocytic processes course between nerve fibers to form septae that partially segregate the fibers into bundles, and their processes form a glial limiting membrane on the outside of the nerve. In old optic nerves the astrocytes hypertrophy, their processes fill spaces produced by the age-related loss of nerve fibers, and some astrocytes come to contain phagocytosed material. Microglial cells in the optic nerve are phagocytes and with age develop many lysosomes and phagosomes.

One might expect that the population of neuroglial cells would decline with age as optic nerve fibers are lost, because the most numerous neuroglial cells are the oligodendrocytes that form the myelin sheaths around the axons. However, the opposite is true. On average, the ratio of neuroglial cell profiles to nerve fiber profiles is more than doubled in the old animals. This doubling is not the result of the cross-sectional area of the optic nerve shrinking with age while the population of neuroglial cells remains static, because the *total* number of neuroglial profiles per section is greater in the old nerves, and the cross-sectional area of the old optic nerves is not significantly smaller. These results are reminiscent of studies of human cortex in which, relative to the neuronal cell population, the putative neuroglial cell population has been reported to increase substantially with age (Brizzee et al., 1975; Terry et al., 1987).

At the same time, there is considerable variation among the optic nerves of the old monkeys in the numbers of nerve fibers and neuroglial cell profiles. All of the nerves from old animals exhibit some degree of myelin abnormality and neuroglial cell involvement, but a few old nerves are relatively unaffected. In the latter, the numbers of nerve fibers and neuroglial profiles are within the range of the young animals. However, most old nerves had fewer nerve fibers and more neuroglial profiles than young nerves, and a few old nerves, not the oldest in our sample, show severe depletion of nerve fibers and an enrichment of microglial cells. Because so little clinical data is available to us, we cannot rule out the possibility that age-related eye disease makes some contribution to the changes we observe in the optic nerve, particularly in the most affected animals, although all of the animals were skilled and successful at behavioral tasks that are based on visual discrimination (Killiany et al., 2000). Despite the individual variations, each neuroglial cell type responds in a characteristic and predictable way as the optic nerve ages, as discussed below.

Astrocytes

Astrocytes account for approximately 35% of the neuroglial nuclear profiles in the young optic nerve, the same proportion found in primary visual cortex in the young monkey (Peters et al., 1991b). They perform myriad functions in the normal brain and optic nerve. Astrocytes form the glial limiting membrane around blood vessels and at the outer surface of the brain and optic nerve; they take up and metabolize neurotransmitters; and they produce cytokines (reviewed by Ridet et al., 1997; Aschner, 1998; Partridge, 1999; Anderson and Swanson, 2000). They react to traumatic injury and normal aging with a response that typically includes hypertrophy, increased expression of GFAP, and sometimes proliferation (reviewed by Schipper, 1996; Ridet et al., 1997; Tacconi, 1998).

With age, the somata and the nuclei of the astrocytes in the optic nerve become larger, but as far as we can determine, the astrocytes do not become more numerous. Three processes could bring about the increase in size of the perikarya: mechanical swelling during tissue processing, pathological swelling as a result of a loss of ionic homeostasis, or hypertrophy. In the first two cases excess fluid accumulates within the astrocyte, so that the cytoplasm appears pale and organelles are more dispersed. We did observe astrocytic processes with this appearance (e.g., Figs. 8 and 9), and it should be noted that a common cause of such a swollen appearance is poor fixation (Peters et al., 1991b). It is indeed difficult to achieve optimal fixation of the optic nerve (Sandell and Peters, 2001). However, pale astrocyte processes are sometimes observed in optic nerves that are otherwise relatively well fixed, and astrocytic swelling is a well-known reaction to glutamate exposure (von Blankenfeld et al., 1995) and brain trauma (Kimelberg, 1995). Such swelling may have toxic consequences if it results in an increased release of glutamate into the extracellular space (Kimelberg, 1995), because excessive glutamate is known to be toxic to oligodendrocytes (reviewed by Matute et al., 2001).

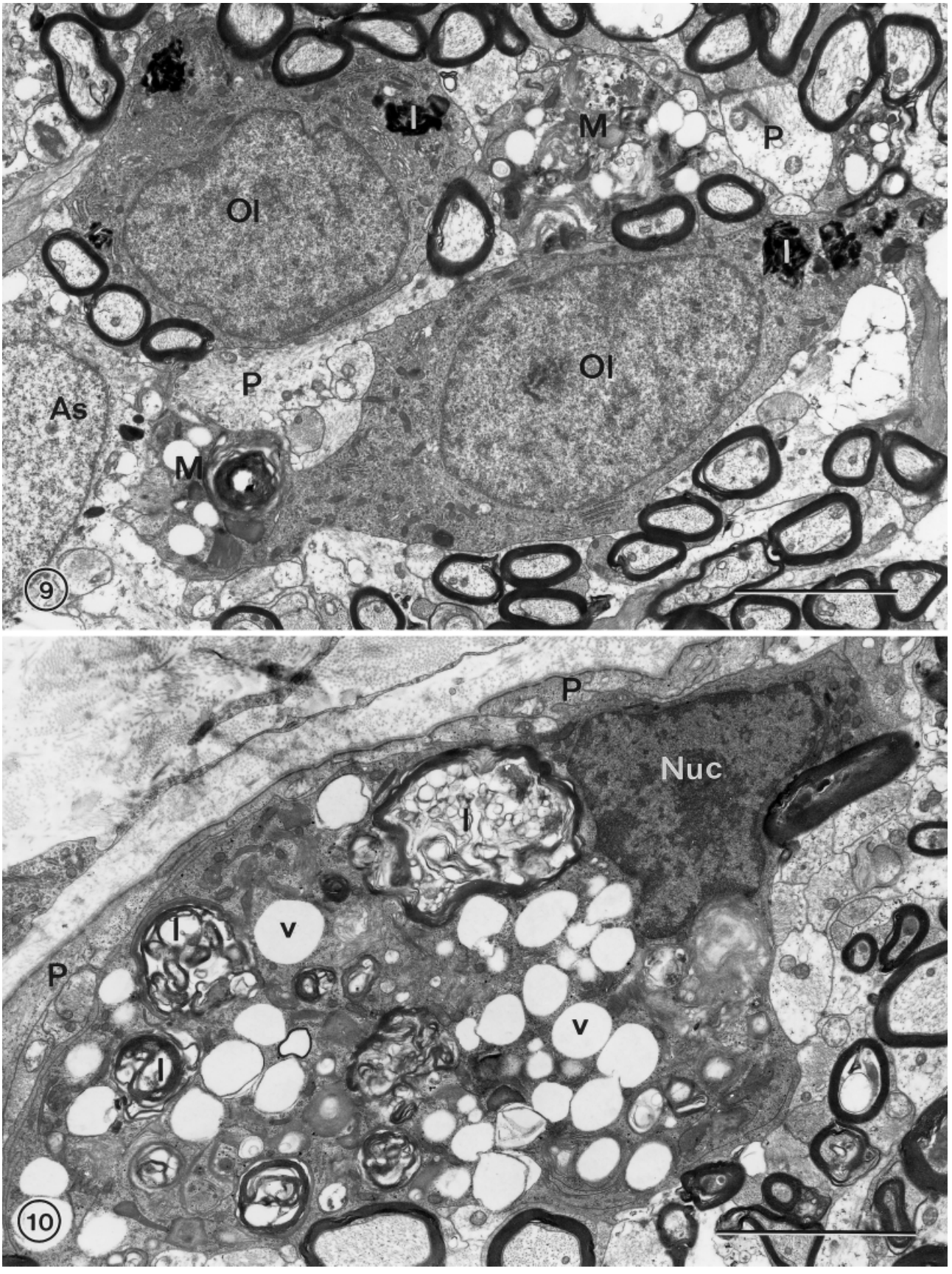

Figures 9–10

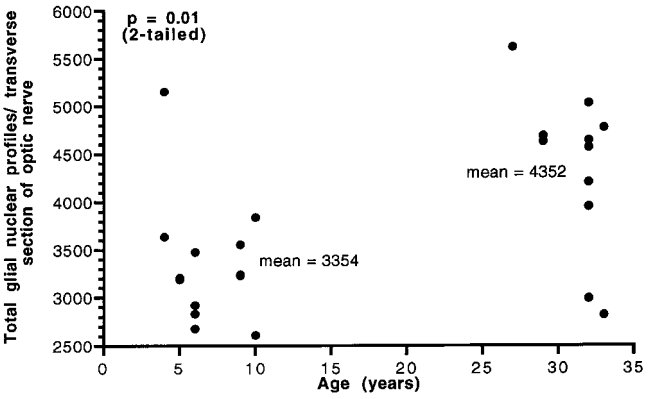

Fig. 11. Scatterplot of the total number of neuroglial nuclear profiles per transverse section of the rhesus monkey optic nerve as a function of age. Values for the two nerves from some animals are so similar to one another (see Table 1) that individual data points overlie each other. The significance (*P*) value for the group means was determined using the mixed linear models analysis, which takes into account the within-subject correlation that is present when data are obtained from both nerves for most animals.

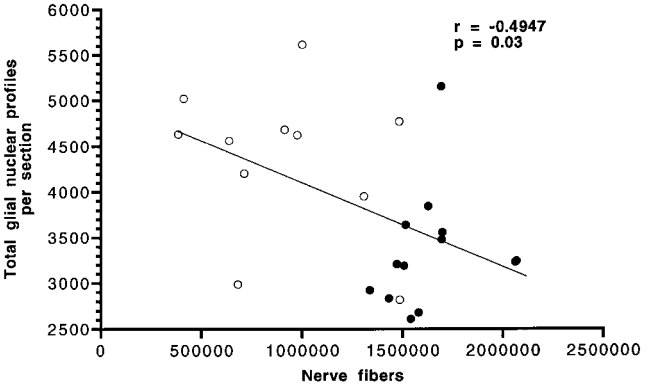

Fig. 12. Regression analysis of the total number of neuroglial nuclear profiles per transverse section of the rhesus monkey optic nerve vs. the number of nerve fibers. Data from old animals are depicted by open circles, and data from young animals are depicted by closed circles. Although all data points are plotted and were used to generate the correlation coefficient (*r*), the significance (*P*) value was determined using the mixed linear models analysis, which takes into account the within-subject correlation that is present when data are obtained from both nerves for most animals.

In astrocytic hypertrophy, the perikarya of the cells become larger, they develop abundant processes, and their processes show an increased number of filaments. We have observed astrocytic changes that resemble hypertrophy, particularly in old nerves in which the nerve fiber number is reduced (e.g., Figs. 2 and 8). Similar changes have been noted in the aging monkey cerebral cortex (Peters et al., 1991b; Peters et al., 1998). This increased production of filaments is reflected in the elevated levels of GFAP that have been noted in aging astrocytes elsewhere in the brain (de la Roza et al., 1985; Berciano et al., 1995; Morgan et al., 1999; Sloane et al., 2000), and it is a hallmark of the astrocytic response to various brain insults (reviewed by Eng et al., 2000).

Although astroglial hyperplasia (hypertrophy and proliferation) characterizes the response of astrocytes to acute traumatic injury and ischemia in the brain (reviewed by Kraig et al., 1995; Norton, 1999), there is no evidence of astroglial proliferation in the aging optic nerve. Perhaps the explanation for the absence of astroglial proliferation in the aging nerve is the absence of mechanical trauma, because this proliferation is most often described as a reaction to a nerve cut or crush. Studies of astrocyte proliferation in the normal aging brain give

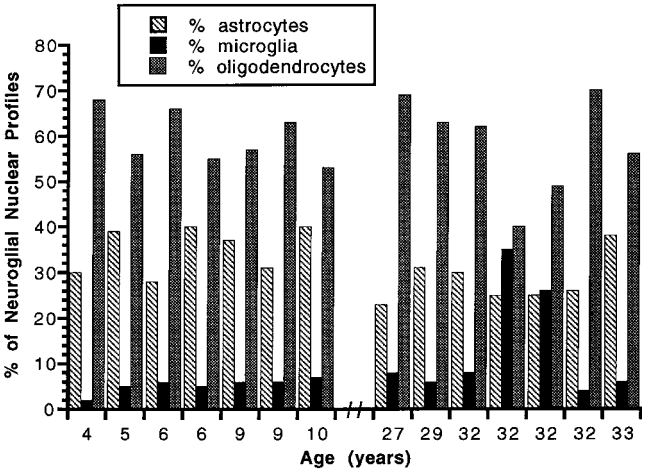

Fig. 13. Histogram showing the proportions of neuroglial nuclei in seven young and seven old optic nerves that were ascribed to astrocytes, microglia, or oligodendrocytes. The identities of the individual animals may be found in Table 1.

Fig. 9. Electron micrograph showing two oligodendrocytes (Ol) in the optic nerve of a 32-year-old monkey, AM 041. In old monkeys it is common for the cytoplasm of oligodendrocytes to contain dense inclusions (I). This micrograph also shows portions of two microglial cells (M) that contain phagocytosed debris, as well as part of the cell body of an astrocyte (As) and astrocytic processes (P). Scale bar = 5 μm.

Fig. 10. Electron micrograph of a microglial cell in the optic nerve of a 32-year-old monkey, AM 041. In this microglial cell the irregularly shaped nucleus (Nuc) is located to one side of the voluminous cell body, which contains clear vacuoles (v), as well as lamellar inclusions (I) that appear to be derived from phagocytosed myelin sheaths. Note the astrocytic processes (P) of the glial limiting membrane. Scale bar = 5 μm.

conflicting results depending on the brain region being examined, counting method, and species. With age the numbers of astrocytes have been reported to decrease in white matter of the cerebellum (Sabbatini et al., 1999); remain unchanged in grey matter of area 17 and in subcortical white matter (Peters et al., 1991b; Sloane et al., 2000); and increase or remain unchanged in the CA1 subfield of the hippocampus (Amenta et al., 1998; Long et al., 1998).

Astrocytes, like the other neuroglial cells in the optic nerve, develop characteristic inclusions within their cytoplasm as they age. The origin of this material is unclear, although astrocytes in the rat brain are known to be phagocytic when presented with degenerating axon termi-

nals (Feldman, 1976) or degenerating myelinated axons (de la Roza et al., 1985).

Oligodendrocytes

Oligodendrocytes produce the myelin sheaths that surround every retinal ganglion cell axon in the primate optic nerve. They are the most common neuroglial cell type in the optic nerve, accounting for approximately 60% of the total glial profiles in transverse sections, similar to the proportion present in monkey primary visual cortex (57.3%, Peters et al., 1991b). The age-related changes in the oligodendrocytes in the optic nerve are also similar to those that have been reported for the cerebral cortex (Peters et al., 1991b; Peters, 1996), with the most prominent change being the increased presence of electron-dense inclusions within the cytoplasm of the cells, and within swellings of their processes.

We have recently described the age-related changes in the myelin sheaths formed by the oligodendrocytes in the optic nerve (Sandell and Peters, 2001), and they can be summarized as follows: 1) Some sheaths are split at the intraperiod line to enclose a fluid-filled vesicle (myelin balloons); 2) other sheaths are separated at the major dense line to accommodate electron-dense cytoplasm that must originate from the parent oligodendrocyte; and 3) in fibers in which the axonal component has degenerated, the myelin sheath is collapsed and disorganized. The first two changes have also been reported for other parts of the normal aging nervous system where degeneration of nerve fibers is not pronounced (Feldman and Peters, 1998; Nielsen and Peters, 2000; Peters et al., 2000). It seems inevitable that even mild myelin disruptions would interfere with axonal conduction, and indeed the median conduction velocity of axons in the pyramidal tract of old cats is 43% slower than in young cats (Xi et al., 1999). Myelin abnormalities in the visual system may contribute to the age-related slowing of the visual evoked response, despite preservation of response amplitude in human observers (Celesia and Daly, 1977).

Each oligodendrocyte typically provides myelin to several nerve fibers (Peters et al., 1991a), so it was not obvious to us what effect the age-related loss of optic nerve fibers would have on the number of oligodendrocytes. Our data suggest that at least two processes are at work: when nerve fiber loss is moderate, the number of oligodendrocytes actually increases, but when the population of nerve fibers falls below about 900,000, the number of oligodendrocytes declines (the average young nerve has 1.6 million nerve fibers). The source of the additional oligodendrocytes is most likely the oligodendrocyte progenitor cells (OPCs), which continue to produce oligodendrocytes even in the adult nervous system (Levison et al., 1999; Levine et al., 2001). Oligodendrocytes are often found in clusters in the old optic nerves, an arrangement that is also common in the white matter of the aging brain (Peters, 1996), and OPCs could give rise to these clusters. We do not yet know what aspect of axon loss or myelin disruption might trigger OPCs to give rise to oligodendrocytes in the aging nerve.

The reduction in the number of oligodendrocyte nuclear profiles in the few nerves with extensive nerve fiber loss might occur because so few axons remain to be myelinated, or because axonal degeneration triggers the generation of toxic cytokines by other neuroglial cells (Merrill et al., 1993; Mitrovic et al., 1994; Hisahara et al., 1997; Matute et al., 2001). Our total sample of old optic nerves is small, and most do not show severe degeneration, so studies of additional optic nerves and other myelinated fiber tracts are needed to address the issue of the relationship between nerve fibers and oligodendrocytes and their interactions during aging.

Microglia

The microglial cell is the least common and least conspicuous cell in the young optic nerve. Microglial cells account for about 6% of the total neuroglial profiles in the young optic nerve, and the proportion increases slightly in the old nerve. These values agree with those obtained in the monkey primary visual cortex (Peters et al., 1991b). The exception to this pattern is provided by the two nerves from the old monkey with abundant axonal degeneration, namely, AM 041 (see Table 1). In these nerves 26% and 35% of the neuroglial profiles were microglia, and the estimated number of microglial nuclear profiles per section was about five times greater than that of the other old nerves. This increase in frequency and the morphological changes shown by these cells are both consistent with microglial activation, which most likely occurs in response to axonal degeneration (reviewed by Kreutzberg et al., 1997). When activated microglia have been found in the normal aging brain, they have been more common in the white matter than in the grey matter (Sheffield and Berman, 1998; Sloane et al., 1999). The severely affected old optic nerves may represent the blossoming of a second stage in the aging process in which there are so many degenerating nerve fibers that the microglial population is greatly expanded to clear the debris. Similar microglial activation occurs in the cerebral cortex in Alzheimer's disease (McGeer et al., 1988), and the resulting release of proinflammatory cytokines by microglial cells has been postulated to contribute to the disease (Banati and Beyreuther, 1995; Unger, 1998).

Not only do the microglia increase in number in some of the old optic nerves, but with age and the ensuing degeneration of nerve fibers, many microglial cells become enlarged and engorged with debris. The most engorged microglial cells were observed in the nerves showing most fiber degeneration, suggesting that it is the degeneration of nerve fibers that activates the microglial cells. Similar microglial activation has been reported in the brains of aging humans (DiPatre and Gelman, 1997; Sheng et al., 1998) and monkeys (Peters et al., 1991b; Peters, 1999). The biochemical signs of microglial activation that have been detected in the aging human and/or monkey brain include increased expression of MHC class II (HLA-DR) antigens (Sheffield and Berman, 1998; Sloane et al., 1999), interleukin-1α (Sheng et al., 1998), and inducible nitric oxide synthase (Sloane et al., 1999), and the aging monkey optic tract contains abundant HLA-DR-positive microglia (T. Kemper, personal communication). Activated microglial cells are well known for the production of potentially destructive cytokines including tumor necrosis factor-α and reactive forms of oxygen and nitrogen (reviewed by Sloane et al., 1999; Matute et al., 2001). These cytokines may be toxic to oligodendrocytes and astrocytes, as well as stimulatory to the microglial cells themselves.

In summary, the morphological changes that are observed in the neuroglial cells in the aging optic nerve are qualitatively similar to those observed elsewhere in the aging central nervous system. In the optic nerve, these

changes are exacerbated by the gradual degeneration of the retinal ganglion cell axons that comprise the nerve (Harman et al., 2000). Thus, in the nerve, the neuroglial cells are presented not only with degenerating myelin, which is ubiquitous in the aging brain, but also with degenerating nerve fibers. In the nerves most affected by age, this nerve fiber degeneration may stimulate the production of cytokines by microglial cells and astrocytes, which has the dual action of further stimulating those cells in an autocrine fashion, as well as acting directly on oligodendrocytes to bring about additional myelin disruption. Although oligodendrocyte somata exhibit the least in the way of morphological changes in the aging optic nerve, the effects of age on the myelin they produce is likely to be of the utmost importance to the normal function of the optic nerve, and ultimately the entire visual system.

ACKNOWLEDGMENTS

The authors thank Ms. Claire Folger for expert technical and photographic assistance and Dr. Howard Cabral of the Boston University School of Public Health for performing the mixed linear models analysis and for valuable discussion of statistical issues.

LITERATURE CITED

Albert MS. 1993. Neuropsychological and neurophysiological changes in healthy adult humans across the age range. Neurobiol Aging 14:623–625.

Amenta F, Bronzetti E, Sabbatini M, Vega J. 1998. Astrocyte changes in aging cerebral cortex and hippocampus: a quantitative immunohistochemical study. Microsc Res Tech 43:29–33.

Anderson C, Swanson R. 2000. Astrocyte glutamate transport: review of properties, regulation, and physiological functions. Glia 32:1–14.

Aschner M. 1998. Astrocytes as mediators of immune and inflammatory responses in the CNS. Neurotoxicology 19:269–281.

Balazsi AG, Rootman J, Drance SM, Schulzer M, Douglas GR. 1984. The effect of age on the nerve fiber population of the human optic nerve. Am J Ophthalmol 97:760–766.

Banati R, Beyreuther K. 1995. Alzheimer's disease. In: Kettenmann H, Ransom BR, editors. Neuroglia. New York: Oxford University Press. p 1027–1043.

Berciano M, Andres M, Calle E, Lafarga M. 1995. Age-induced hypertrophy of astrocytes in rat supraoptic nucleus: a cytological, morphometric, and immunocytochemical study. Anat Rec 243:129–144.

Brizzee K, Klara P, Johnson J. 1975. Changes in microanatomy, neurocytology and fine structure with aging. In: Ordy J, Brizzee K, editors. Neurobiology of aging. New York: Plenum Press. p 575–594.

Celesia G, Daly R. 1977. Effects of aging on visual evoked responses. Arch Neurol 34:403–407.

de la Roza C, Cano J, Reinoso-Suarez F. 1985. An electron microscopic study of astroglia and oligodendroglia in the lateral geniculate nucleus of aging rats. Mech Ageing Dev 29:267–281.

Diggle PJ, Liang KY, Zeger SL. 1994 Analysis of longitudinal data. Oxford: Clarendon Press.

DiPatre P, Gelman B. 1997 Microglial cell activation in aging and Alzheimer disease: partial linkage with neurofibrillary tangle burden in the hippocampus. J Neuropathol Exp Neurol 56:143–149.

Eng L, Ghirnikar R, Lee Y. 2000. Glial fibrillary acidic protein: GFAP—thirty-one years (1969–2000). Neurochem Res 25:1439–1451.

Feldman ML. 1976. Aging changes in the morphology of cortical dendrites. In: Terry RD, Gershon S, editors. Neurobiology of aging. New York: Raven Press. p 211–227.

Feldman ML, Peters A. 1998. Ballooning of myelin sheaths in normally aged macaques. J Neurocytol 27:605–614.

Guttmann CRG, Jolesz FA, Kikinis R, Killiany RJ, Moss MB, Sandor T, Albert MS. 1998. White matter changes with normal aging. Neurology 50:972–978.

Harman A, Abrahams B, Moore S, Hoskins R. 2000. Neuronal density in the human retinal ganglion cell layer from 16–77 years. Anat Rec 260:124–131.

Hisahara S, Shoji S, Okano H, Miura M. 1997. ICE/CED-3 family executes oligodendrocyte apoptosis by tumor necrosis factor (TNF). J Neurochem 69:10–20.

Jonas JB, Schmidt AM, Muller-Bergh JA, Schlotzer-Schrehardt UM, Naumann GOH. 1992. Human optic nerve fiber count and optic disk size. Invest Ophthalmol Vis Sci 33:2012–2018.

Killiany RJ, Moss MB, Rosene DL. Recognition memory function in early senescent rhesus monkeys. Psychobiology 28:45–56.

Kimelberg H. 1995. Brain edema. In: Kettenmann H, Ransom BR, editors. Neuroglia. New York: Oxford Press. p 919–935.

Kraig R, Lascola C, Caggiano A. 1995. Glial response to brain ischemia. In: Kettenmann H, Ransom BR, editors. Neuroglia. New York: Oxford Press. p 964–976.

Kreutzberg G, Blakemore W, Graeber M. 1997. Cellular pathology of the central nervous system. In: Graham D, Lantos P, editors. Greenfield's neuropathology. London: Arnold. p 85–156.

Lai ZC, Rosene DL, Killiany RJ, Pugliese D, Albert MS, Moss MB. 1995. Age-related changes in the brain of the rhesus monkey: MRI changes in white matter but not grey matter. Soc Neurosci Abstr 21:1564.

Levine J, Reynolds R, Fawcett J. 2001. The oligodendrocyte precursor cell in health and disease. Trends Neurosci 24:39–47.

Levison S, Young G, Goldman J. 1999. Cycling cells in the adult rat neocortex preferentially generate oligodendroglia. J Neurosci Res 57: 435–446.

Linnemann D, Skarsfelt T. 1994. Regional changes in expression of NCAM, GFAP, and S100 in aging rat brain. Neurobiol Aging 15:651–655.

Long J, Kalehua A, Muth N, Calhoun M, Jucker M, Hengemihle J, Ingram D, Mouton P. 1998. Stereological analysis of astrocyte and microglia in aging mouse hippocampus. Neurobiol Aging 19:497–503.

Matute C, Alberdi E, Domercq M, Perez-Cerda F, Perez-Samartin A, Sanchez-Gomez M. 2001. The link between excitotoxic oligodendroglial death and demyelinating diseases. Trends Neurosci 24:224–230.

McGeer P, Itagaki S, McGeer E. 1988. Expression of histocompatibility glycoprotein HLA-DR in neurological disease. Acta Neuropathol 76: 550–557.

Merrill J, Ignarro L, Sherman M, Melinek J, Lane T. 1993. Microglial cell cytotoxicity of oligodendrocytes is mediated through nitric oxide. J Immunol 151:2132–2141.

Mikelberg FS, Drance SM, Schulzer M, Yidegiligne HM, Weis MM. 1989. The normal human optic nerve. Ophthalmology 96:1325–1328.

Mitrovic B, Ignarro L, Montestruque S, Smoll A, Merrill J. 1994. Nitric oxide as a potential pathological mechanism in demyelination: its differential effects on primary glial cells in vitro. Neuroscience 61:575–585.

Morgan T, Xie Z, Goldsmith S, Yoshida T, Lanzrein A, Stone D, Rozovsky I, Perry G, Smith M, Finch C. 1999. The mosaic of brain glial hyperactivity during normal ageing and its attenuation by food restriction. Neuroscience 89:687–699.

Morrison JC, Cork LC, Dunkelberger GR, Brown A, Quigley HA. 1990. Aging changes of the rhesus monkey optic nerve. Invest Ophthalmol Vis Sci 31:1623–1627.

Nielsen K, Peters A. 2000. The effects of aging on the frequency of nerve fibers in rhesus monkey striate cortex. Neurobiol Aging 21:621–628.

Norton W. 1999. Cell reactions following acute brain injury: a review. Neurochem Res 24:213–218.

Partridge W. 1999. Blood-brain barrier biology and methodology. J Neurovirol 5:556–569.

Peters A. 1996. Age-related changes in oligodendrocytes in monkey cerebral cortex. J Comp Neurol 371:163–163.

Peters A. 1999. Normal aging in the cerebral cortex of primates. In: Peters A, Morrison JH, editors. Cerebral cortex, vol 14. New York: Kluwer Academic/Plenum Press. p 49–80.

Peters A, Palay SL, Webster H. 1991a. The fine structure of the nervous system. New York: Oxford University Press.

Peters A, Josephson K, Vincent SL. 1991b. Effects of aging on the neuroglial cells and pericytes within area 17 of the rhesus monkey cerebral cortex. Anat Rec 229:384–398.

Peters A, Leahu D, Moss MB, McNally KJ. 1994. The effects of aging on area 46 of the frontal cortex of the rhesus monkey. Cereb Cortex 6:621–635.

Peters A, Leahu D, Moss MB, McNally KJ. 1998. The effects of aging on

layer 1 in area 46 of prefrontal cortex in the rhesus monkey. Cereb Cortex 8:671–684.

Peters A, Moss MB, Sethares C. 2000. Effects of aging on myelinated nerve fibers in monkey primary visual cortex. J Comp Neurol 419:364–376.

Ridet J, Malhotra S, Privat A, Gage FH. 1997. Reactive astrocytes: cellular and molecular cues to biological function. Trends Neurosci 20:570–577.

Sabbatini M, Barili P, Bronzetti E, Zaccheo D, Amenta F. 1999. Age-related changes of glial fibrillary acidic protein immunoreactive astrocytes in the rat cerebellar cortex. Mech Ageing Dev 108:165–172.

Sandell J, Peters A. 2001. Effects of age on nerve fibers in the rhesus monkey optic nerve. J Comp Neurol 429:541–553.

Schipper H. 1996. Astrocytes, brain aging, and neurodegeneration. Neurobiol Aging 17:467–480.

Sheffield LG, Berman NEJ. 1998. Microglial expression of MHC class II increases in normal aging of nonhuman primates. Neurobiol Aging 19:47–55.

Sheng J, Mrak R, Griffin W. 1998. Enlarged and phagocytic, but not primed, interleukin-1 (IL-1) alpha-immunoreactive microglia increase with age in normal human brain. Acta Neuropathol 95:229–234.

Sloane J, Hollander W, Moss M, Rosene D, Abraham C. 1999. Increased microglial activation and protein nitration in white matter of the aging monkey. Neurobiol Aging 20:395–405.

Sloane JA, Hollander W, Rosene DL, Moss MB, Kemper T, Abraham CR. 2000. Astrocytic hypertrophy and altered GFAP degradation with age in subcortical white matter of the rhesus monkey. Brain Res 862:1–10.

Tacconi M. 1998. Neuronal death: is there a role for astrocytes? Neurochem Res 23:759–765.

Tang Y, Nyengaard JR, Pakkenberg B, Gundersen HJG. 1997. Age-induced white matter changes in the human brain: a stereological investigation. Neurobiol Aging 18:609–615.

Terry RD, DeTeresa R, Hansen LA. 1987. Neocortical cell counts in normal human adult aging. Ann Neurol 21:530–539.

Unger J. 1998. Glial reaction in aging and Alzheimer's disease. Microsc Res Tech 43:24–28.

von Blankenfeld G, Enkvist K, Kettenmann H. 1995. Gamma-aminobutyric acid and glutamate receptors. In: Kettenmann H, Ransom BR, editors. Neuroglia. New York: Oxford Press. p 335–345.

West MJ, Ostergaard K, Anreassen OA, Finsen B. 1996. Estimation of the number of somatostatin neurons in the striatum: an in situ hybridization study using the optical fractionator method. J Comp Neurol 370: 11–22.

Xi M-C, Liu R-H, Engelhardt K, Morales F, Chase M. 1999. Changes in the axonal conduction velocity of pyramidal tract neurons in the aged cat. Neuroscience 92:219–225.